

Novel Compact Harmonic-Rejected Ring Resonator Based Bandpass Filter

Tamer G. Abouelnaga^{1, *} and Ashraf S. Mohra²

Abstract—In this paper, a novel compact ring resonator based bandpass filter with a second harmonic rejection capability is proposed. The proposed bandpass filter uses a stepped-impedance open stubs and a stepped-impedance ring resonator at feeding lines. Stepped-impedance open stubs are used to obtain a better rejection level in the second harmonic-frequency band. Ring resonator's radius is calculated by examining and solving the eigenvalue equation of the ring resonator. Firstly, Sierpinski second order curve is used to achieve size reduction of about 66% and 71% compared to conventional microstrip ring bandpass filter inner and outer areas, respectively. Sierpinski curve is chosen because of its symmetry and its suitability for orthogonal feeding lines and open stubs incorporation without using any additional space. Referring to resonant rejection value, the proposed first Sierpinski structure -15 dB simulated fractional bandwidth is 5.6% at 1.505 GHz and with rejection of -0.16 dB. Transmission zeros at 2.25 GHz and 3.78 GHz are obtained. Secondly, stepped-impedance open stubs are added to the resonator ports to add another transmission zero at 3.84 GHz. At 2.9 GHz, second harmonic band, the proposed structure achieves rejection of -6.7 dB instead of -1.7 dB for the conventional one. The proposed structure -15 dB simulated fractional bandwidth is 3% at 1.42 GHz. Innovation is achieved by the simplicity of inserting the transmission zeros, controlling zeros rejection values, incorporating stubs and orthogonal feeding lines in the same resonator area and reasonable power capability of the proposed structure. The proposed bandpass filter's prototype is fabricated using FR4 material, and a good agreement is found between simulated and measured results for return loss and rejection values. The proposed structure is very suitable for L-band applications.

1. INTRODUCTION

Bandpass filters (BPFs), especially ring resonator based ones, are essential components in microwave front end. The microstrip ring resonator has been widely used in microwave couplers, mixers bandpass filters, oscillators, and antennas development [1].

In general, microwave components must achieve linearity, harmonics rejection, miniaturized size and an acceptable noise figure. These requirements have been achieved by the ring resonator based filter [2–6]. Many miniaturization methods were proposed, such as using a $\lambda/4$ broadside-coupled microstrip-to-coplanar waveguide section to substitute the $3\lambda/4$ -section of the conventional ring [7]. This method saves 80% of the area, but it has two main disadvantages, complex structure and partial ground plane which limits the integration of active components' number on the same surface. Miniaturized ring resonator bandpass filter was implemented in [8]. It was implemented by cascading several microwave C-sections. It occupied 30% of the area of a traditional ring resonator BPF. The main disadvantage of this structure is the second frequency limited tuning range. The miniaturization in [9] was achieved by metallic via-holes and spiral configuration. The circuit size is 20.5% of that of a conventional ring

Received 2 April 2017, Accepted 18 May 2017, Scheduled 2 June 2017

* Corresponding author: Tamer Gaber Mohammed Ali Abouelnaga (tamer@eri.sci.eg).

¹ Microstrip Circuits Department, Electronics Research Institute, Giza, Egypt. ² Benha Faculty of Engineering, Benha University, Qalyubia, Egypt.

resonator but with complex structure and very sensitive design performance to coplanar waveguide gap size. In [10], the miniaturization was achieved by using a spiral trace instead of conventional ring one. The circuit area is 29% of that of a traditional ring. The main disadvantages are the complex structure and sensitivity to the very thin trace width. In [11], a miniaturized ring resonator based BPF was obtained by using broadside-coupled split ring resonator and capacitors. In this method, a size reduction of 27.17% was obtained. The main disadvantages are lumped capacitor and multilayer format.

In [12], two approaches had been used to achieve acceptable levels of space reduction and wave propagation through stubs redesigning and defected ground structures incorporation, respectively [13]. This filter suffered from the existence of a narrow lower stopband. A single mode ring resonator was introduced in [14]. It employed one-wavelength ring resonator coupled to quarter-wavelength line. But the structure suffered from large size. High selectivity 3rd order bandpass filter with harmonic suppression capability was introduced in [15], where complementary split ring resonator was used to achieve a higher selectivity and harmonic suppression. Three complementary split ring resonators were used, and two of them were in series, so its main drawback was its large size.

Most of the previous designs suffer from the presence of harmonics which are naturally excited and can't be avoided. Also, low power capability is another drawback due to thin traces of all previous ring resonator. Some designs make use of harmonics existence in implementing multiple-mode ring resonator. In [16], multiple-mode ring resonator with circuit area of 72% compared to conventional one was implemented. Other designs control the dual modes frequencies through using two short-circuited half-wave stepped-impedance resonators [17] and degenerating the resonant modes [18]. In fact, dual mode ring resonator with sharp rejection capabilities [19–22] has difficulties in adjusting their poles and zeros points. They have tedious electromagnetic wave calculations and are very complex to be implemented [23, 24]. Many designs were proposed [25–28] to extend the passband of the BPF based on the idea of multiple resonance ring resonator.

In this paper, a very simple and low cost stepped-impedance open stubs compact harmonic-rejected BPF is proposed. Eigenvalue equation of the ring resonator is solved to obtain a BPF design curve. Sierpinski second order curve is used, and a size reduction of 71% is obtained. Two identical stepped-impedance open stubs are incorporated to add a new transmission zero at 3.84 GHz. Rejection and return loss are investigated, discussed and compared to their measured counterparts

The proposed BPF is very suitable for L-band applications. L-band frequency extends from 1 to 2 GHz. In Europe, the L-band spectrum from 1452–1492 MHz is dedicated for terrestrial communications networks. The Global Positioning System GPS carriers are centered at 1176.45 MHz (L_5), 1227.60 MHz (L_2), 1381.05 MHz (L_3), and 1575.42 MHz (L_1) frequencies. In United States and overseas territories, the L band is held by the military for telemetry and Digital Audio Broadcasting (DAB) which is typically done in the 1452–1492 MHz range.

The proposed structure novelty is achieved by the structure itself which allows incorporation of stepped impedance open stubs and orthogonal feeding lines without any extra space. Also, the simplicity of controlling the transmission zeros through the curve perimeter and stubs' lengths according to the available space. The proposed structure also shows a reasonable power capability through using FR4 material and suitable microstrip line width.

2. CONVENTIONAL RING RESONATOR BANDPASS FILTER

The microstrip ring resonator is a well-known structure. It is considered as a cavity resonator with electric walls on the top and the bottom, and magnetic walls on the side border. As it had been shown in [3, 29], a solution of Maxwell's equations for the electromagnetic field components were written as

$$\begin{aligned}
 E_Z &= [AJ_n(kr) + BY_n(kr)] \cos(n\theta) \\
 H_r &= \frac{n}{j\omega\mu_0 r} [AJ_n(kr) + BY_n(kr)] \sin(n\theta) \\
 H_\theta &= \frac{k}{j\omega\mu_0} [AJ'_n(kr) + BY'_n(kr)] \cos(n\theta)
 \end{aligned} \tag{1}$$

where J_n , Y_n , J'_n , and Y'_n are n order and argument (kr) Bessel function of first kind, second kind, derivative of first kind, and derivative of second kind, respectively. A and B are constants, and \emptyset is the cylindrical coordinate azimuth angle. The eigenvalue equation of the resonator resulting from the boundary conditions is

$$\frac{J'_n(kr_o) - Y'_n(kr_o)}{J'_n(kr_i) - Y'_n(kr_i)} = 0 \quad k = \omega \sqrt{\epsilon_o \epsilon_r \mu_o} \tag{2}$$

where r_o and r_i are the outer and inner radii of the ring resonator. It can be noticed that cosine and sine functions in Eq. (1) can be replaced by sine and cosine functions, respectively. These fields are also solutions for the field azimuthal angle \emptyset dependence. This means that, at resonance, two degenerate modes are obtained. In symmetrical excitation, only one mode will be excited. Since both modes are orthogonal, there will not be any coupling between the two modes. If the resonator's symmetry is disturbed, the two degenerate modes can be coupled. This can be done if the excitation lines of the resonator are asymmetrically, Fig. 1. As a solution method of Eq. (2), Matlab code is built to obtain all possible solutions.

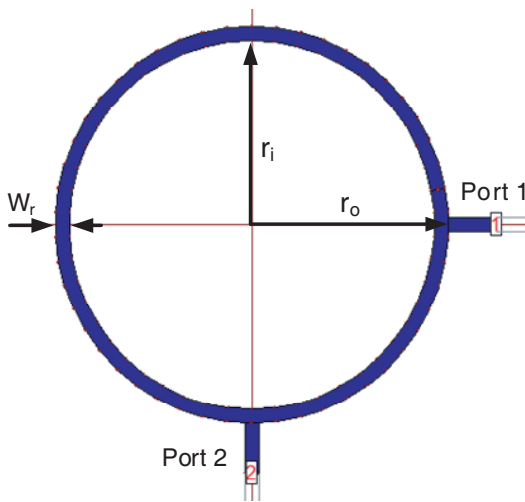


Figure 1. Microstrip ring resonator.

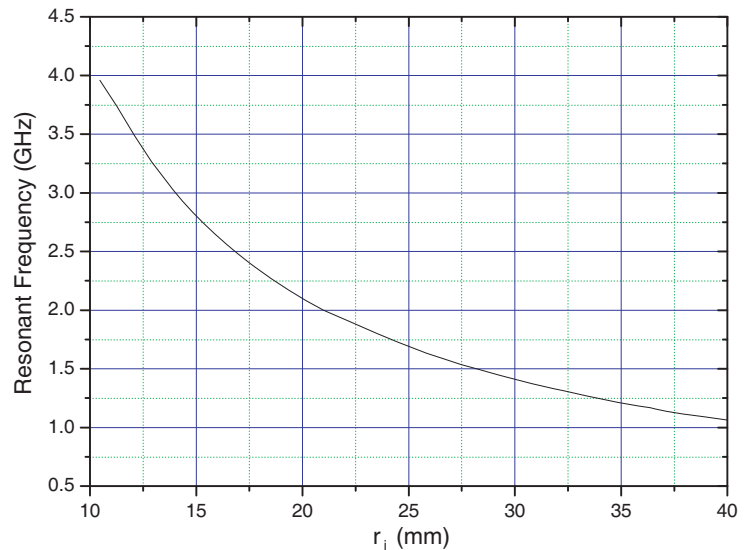


Figure 2. Microstrip ring resonator resonant frequency versus inner radius.

Figure 2 shows the ring resonator resonant frequency and its inner radius relation based on the Matlab solution of Eq. (2) at different inner radii. FR4 material with dielectric constant $\epsilon_r = 4.3$ and thickness of 1.5 mm is used as ring resonator substrate. The 50Ω microstrip ring resonator path width W_r is 2.72 mm, [30] is used. A ring resonator's inner radius of 28 mm is first considered for 1.5 GHz resonant frequency, Fig. 2.

Zeland Software IE3D Version 12 is used as a full wave analysis tool. A resonant frequency of 1.8 GHz is obtained. Increasing the inner radius from 28 mm to 35 mm will bring the resonant frequency back to 1.5 GHz. This difference is referred to the electric and magnetic walls that were assumed in analytical solution. Fig. 1 shows the microstrip ring resonator geometry, and Fig. 3 shows S -parameters of the conventional BPF. The first resonant frequency rejection is -0.9 dB at 1.48 GHz, Fig. 3.

Referred to resonant frequency rejection value, the simulated -3 dB fractional bandwidth is 40.5%, while the simulated -0.1 dB fractional bandwidth is 7.6% with return loss of 15 dB in the same frequency range. Also, another passband appears at resonant frequency of 2.92 GHz with rejection value of -1.8 dB. The fractional -3 dB bandwidth is 17.8%, while the fractional -0.1 dB bandwidth is 3.1% with 15 dB return loss in the same frequency range. The conventional bandpass filter inner ring area is 38.5 cm^2 and its outer ring area is 44.7 cm^2 . The problem arises from the higher order passband (harmonics) and the large area of the conventional BPF.

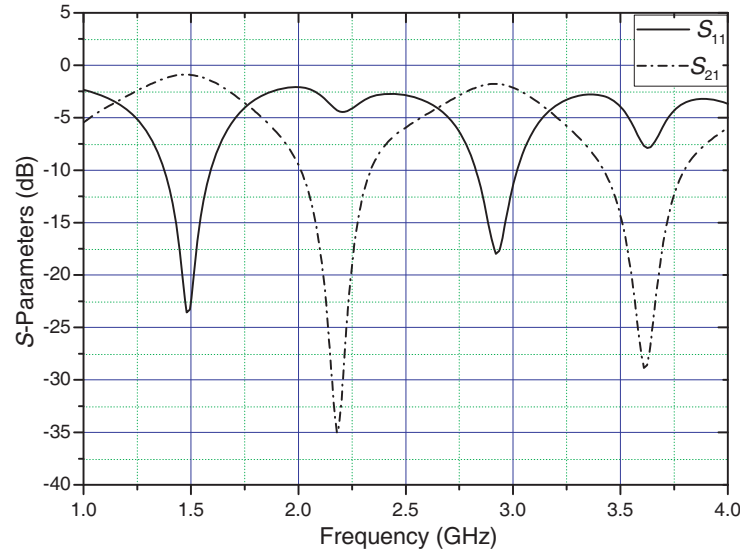


Figure 3. Microstrip ring resonator S -parameters.

3. PROPOSED COMPACT HARMONIC-REJECTED RING RESONATOR BASED BPF

Several mathematicians were interested in continuous but nondifferentiable curves with infinite length and finite occupied area. Cantor probably was the first to describe fractal iteration. Peano, Sierpinski, Hilbert and Koch curves are the most curves that were published in microwave engineering area. Synthesis and design techniques for half-wavelength meandered line filters, Hilbert filters and Minkowski filters were introduced in [31].

Iterative graphics are described by L-systems rather than equations. Replacement is the concept of L-systems. L-systems use alphabets and symbols to express the initial condition, which called axiom. Axiom and production rules of an L-System that generates Sierpinski curves are given by

$$\begin{aligned}
 &\text{Angle } 60 \\
 &\text{Axiom } FX \\
 &F \rightarrow Z \\
 &X \rightarrow +FY - FX - FY + \\
 &Y \rightarrow -FX + FY + FX -
 \end{aligned}$$

In this system, an F or an FX is an instruction to draw a line segment one unit in the current direction, a $+$ is one angular unit counterclockwise instruction, and a $-$ is one angular unit clockwise instruction. Thus for n th iteration the unfolded length of the curve is $(3/2)^n$ [32].

Sierpinski curve is a recursive sequence of continuous closed plane which almost completely fills the unit square. Matlab code is built to draw the Sierpinski curve which will be used to implement the ring resonator. Fig. 4 shows the Sierpinski curve of order 1, 2, 3, and 4, respectively.

Sierpinski curve is the best choice among other fractal curves for compact ring resonator implementation. This is because Sierpinski curves is a closed symmetrical path and it allows orthogonal feeding lines to be incorporated without using any additional space. Also, at the feeding lines positions, there are enough space to add an open stubs which are essential elements for transmission zero appearance. Applying Sierpinski fractal geometry to the conventional ring resonator based BPF design can absolutely shrink its area. Sierpinski curve is also chosen because it has a minimum coupling effect between the adjacent lines. This can be achieved by ensuring that the current paths is in opposite direction at all adjacent lines.

Figure 5 shows the proposed compact microstrip ring resonator based BPF with an area of 12.96 cm^2 . In conventional microstrip ring resonator, the electromagnetic fields were assumed to be

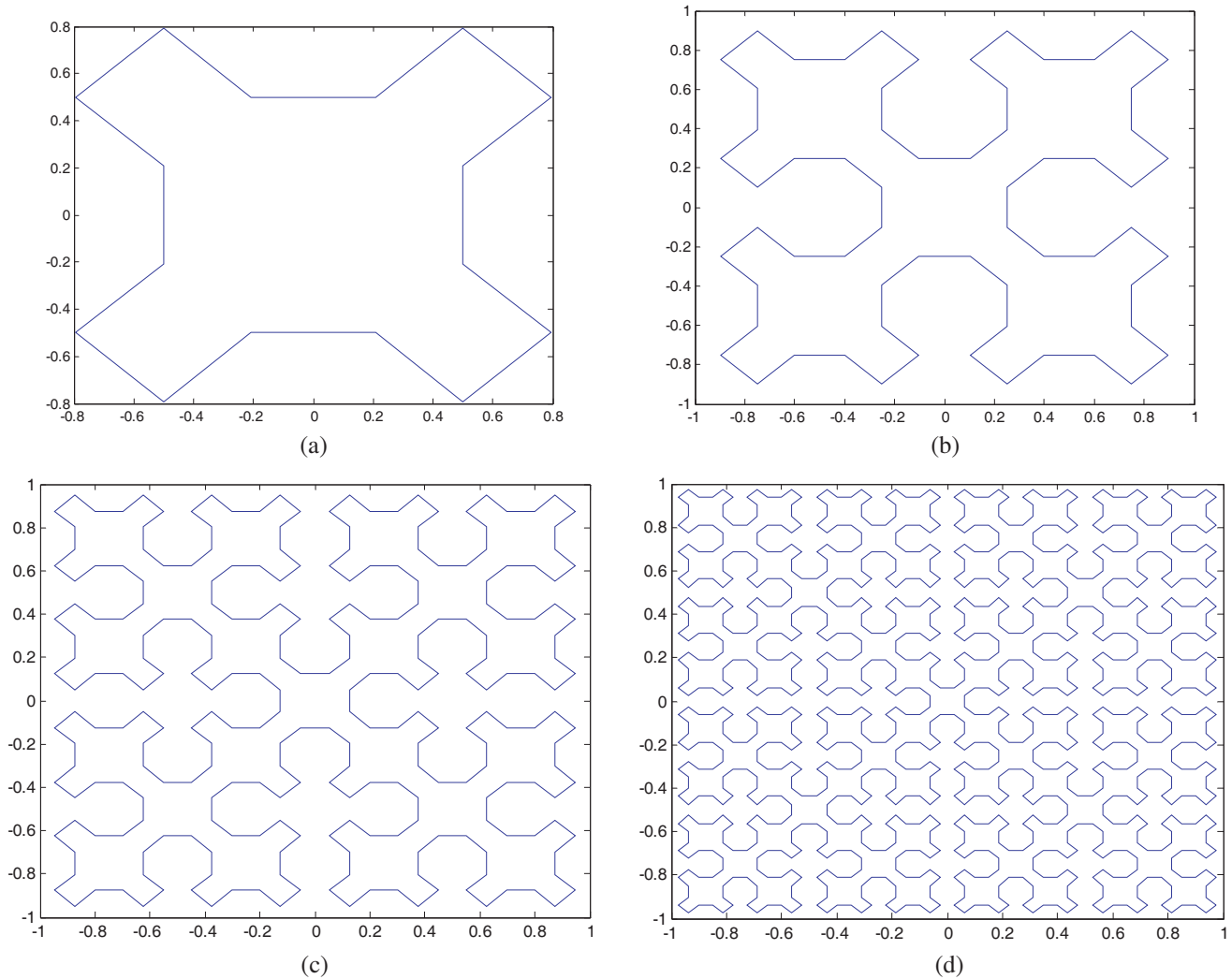


Figure 4. Sierpinski fractal geometry.

TM fields. For the thin substrates, the fields may be taken as independent of the z coordinate (smallest dimension). The fields propagate in the radial direction and have θ variation [3, 29]. The cylindrical geometry of the conventional ring resonator will allow only θ variation at specific value of r . The proposed geometry has different values of r at the same geometry. This makes Maxwell’s equations analytical solutions of such a structure will not be accurate. So, the proposed structure may be approximated to conventional structure with same circumference or may be solved numerically using CST or IE3D simulators.

Figure 6 shows rejection of about -1.1 dB at 1.505 GHz using IE3D simulator. Referred to the resonant rejection value, the simulated -3 dB fractional bandwidth is 31.8%, while the simulated -0.16 dB fractional bandwidth is 5.6% with return loss of 15 dB in the same frequency range. So, as a result of using Sierpinski curve in the proposed structure instead of circular curve in conventional structure, size reduction of 66% and 71% are obtained compared to the inner and outer ring areas of the conventional structure, respectively. As conventional ring resonator BPF suffers from the existence of second harmonic at 2.92 GHz, the proposed structure still suffers from the existence of second harmonic at 2.9 GHz, Fig. 6.

The second harmonic of the proposed BPF is rejected by simply adding two identical tapered stubs at the resonator input (see Fig. 7). Open identical tapered stubs are placed so that transmission zeros can be adjusted, and another transmission zero can be independently created for stopband extension

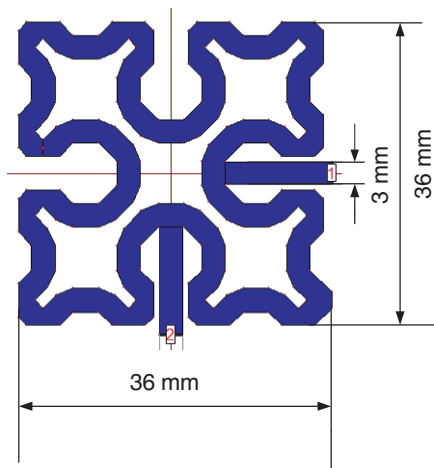


Figure 5. Proposed compact microstrip ring resonator based BPF.

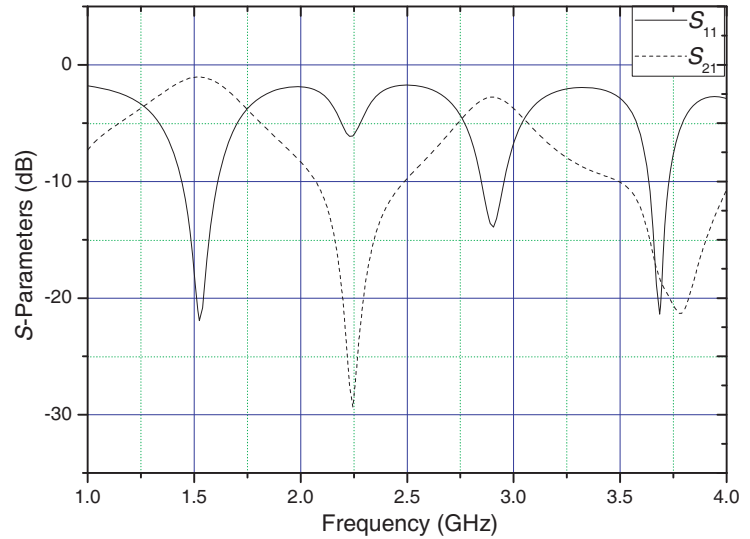


Figure 6. Proposed compact microstrip ring resonator based BPF S -parameters.

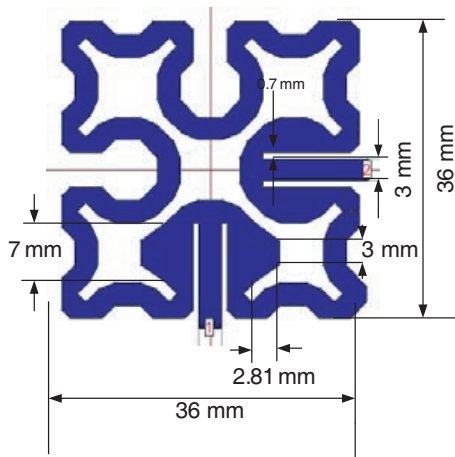


Figure 7. Proposed compact microstrip BPF with higher suppressed passband.

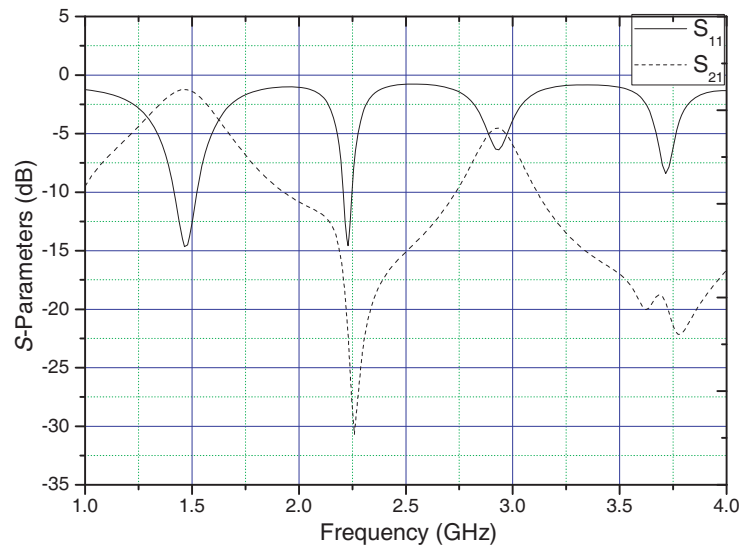


Figure 8. Proposed compact microstrip BPF with higher suppressed passband S -parameters with stubs lengths of 2.81 mm.

and rejection level improvement. Fig. 8 shows that with a tapered open stub length of 2.81 mm, the first transmission zero at 2.25 GHz becomes -30.7 dB (see Fig. 8) instead of -29 dB (see Fig. 6). The second transmission zero at 3.78 GHz becomes -22.2 dB (see Fig. 8) instead of -21.3 dB (see Fig. 6). Fig. 8 shows that a new transmission zero is obtained at 3.63 GHz with rejection level of -20 dB. The new transmission zero mainly refers to the existence of the new two identical open stubs. Also, it can be noticed that the rejection level becomes -4.5 dB at 2.92 (see Fig. 8) instead of -2.8 (see Fig. 6). Fig. 9 shows that by extending the tapered open stub length from 2.81 mm to 6.8 mm, the first transmission zero at 2.25 GHz becomes -36 dB (see Fig. 10) instead of -30.7 dB (see Fig. 8). The second transmission zero at 3.78 GHz becomes -24.8 dB (see Fig. 10) instead of -22.2 dB (see Fig. 8). Also, the new transmission zero becomes -22.3 dB at 3.48 GHz (see Fig. 10) instead of -20 dB at 3.63 GHz (see Fig. 8). This mainly refers to the length extension of the new two identical tapered open stubs

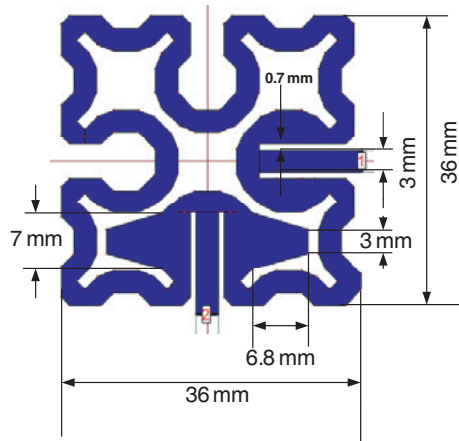


Figure 9. Proposed compact microstrip BPF with higher suppressed passband.

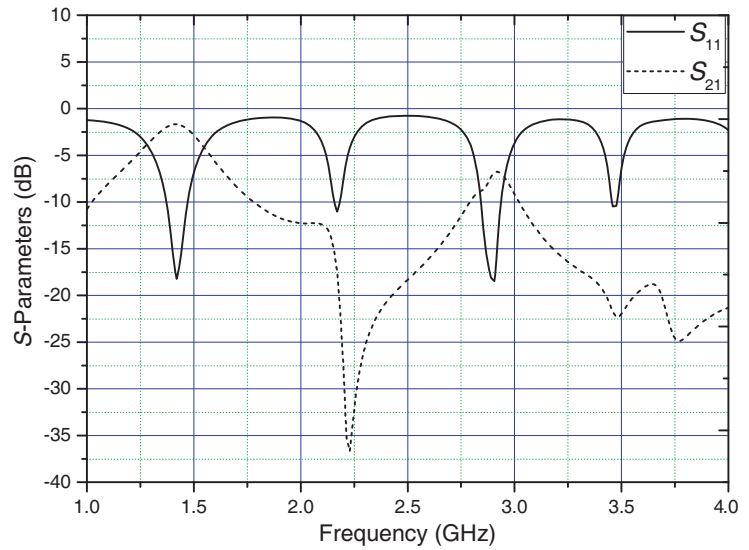


Figure 10. Proposed compact microstrip BPF with higher suppressed passband S -parameters with stubs lengths of 6.8 mm.

Table 1. Comparison among conventional and proposed bandpass filters.

Filter type	Outer area (cm ²)	Outer Perimeter (mm)	Fundamental harmonic		Second harmonic	
			-15 dB fractional BW	Rejection (dB)	-15 dB fractional BW	Rejection (dB)
Conventional BPF (Fig. 1)	44.7	228.5	7.6%	-0.9	3.1%	-1.7
Sierpinski BPF (Fig. 5)	12.96	236.6	5.6%	-1.1	-	-2.7
Sierpinski BPF with 2nd harmonic suppression and stubs lengths of 2.81 mm (Fig. 7)	12.96	236.6	-	-1.6	-	-4.5
Sierpinski BPF with 2nd harmonic suppression and stubs lengths of 6.8 mm (Fig. 9)	12.96	236.6	3%	-1.6	1.7%	-6.7

from 2.81 mm to 6.8 mm. Also, it can be noticed that the rejection level becomes -6.7 dB (see Fig. 10) instead of -4.5 dB (see Fig. 8) at 2.92 GHz. Table 1 shows a comparison among conventional BPF and the proposed three Sierpinski BPF structures.

4. FABRICATION AND MEASUREMENT

Based on the design curve, Fig. 2 and IE3D analysis, 2nd harmonic-rejected ring resonator bandpass filter with a center frequency of 1.42 GHz is chosen to be fabricated and measured. The chosen BPF has -3 dB simulated fractional bandwidth of 18.6% and -1.6 dB simulated rejection fractional bandwidth of 3% with 15 dB return loss in the same frequency band (see Fig. 9). Also, a rejection of -6.7 dB at 2.9 GHz

is obtained. The proposed BPF is fabricated using an FR4 substrate with thickness of 1.5 mm, dielectric constant of 4.3 and loss tangent of 0.025 (see Fig. 11). It is worth to mention that FR4 material dielectric breakdown occurs at 50 kV. The proposed structure's S -parameters are measured using four ports Rohde and Schwarz ZVB 20 vector network analyzer. Fig. 12 shows a comparison between measured and IE3D simulated S -parameters. Good agreement is obtained between measured and simulated results except for a frequency shift of 5.3%. This discrepancy occurs because the proposed structure's substrate and ground plane real sizes are not considered in IE3D simulation process. IE3D simulator is used because it is a very fast full wave analysis tool, and its accuracy is always at an acceptable level. The final design is exported from IE3D to Ansoft CST Microwave Studio 2014 simulator where the proposed structure ground plane and substrate real sizes are considered. Fig. 13 shows the measured and CST simulated S -parameters where a frequency shift of only 3.3% exists between measured and simulated results. One can notice that measured and simulated results are very close to each other when ground plane and substrate finite sizes are considered.

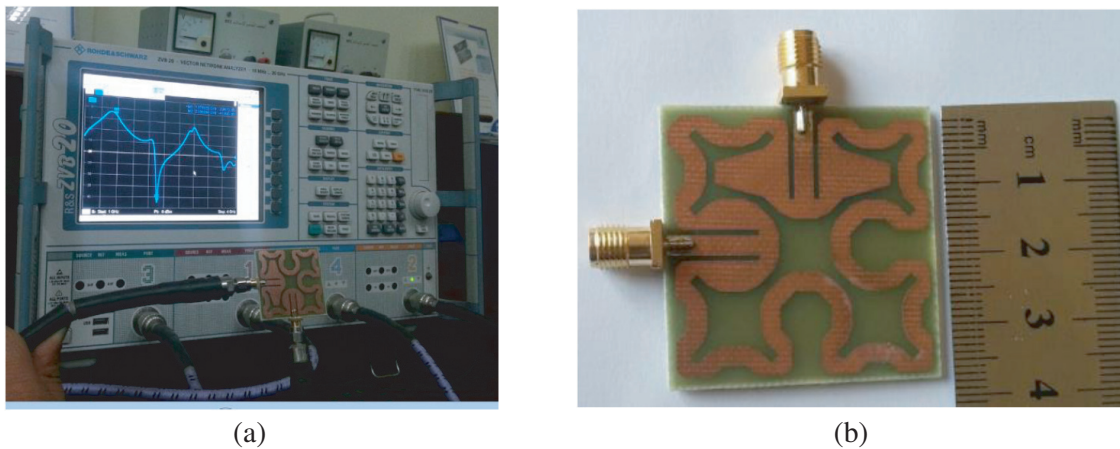


Figure 11. Proposed fabricated harmonic-rejected compact microstrip BPF photo.

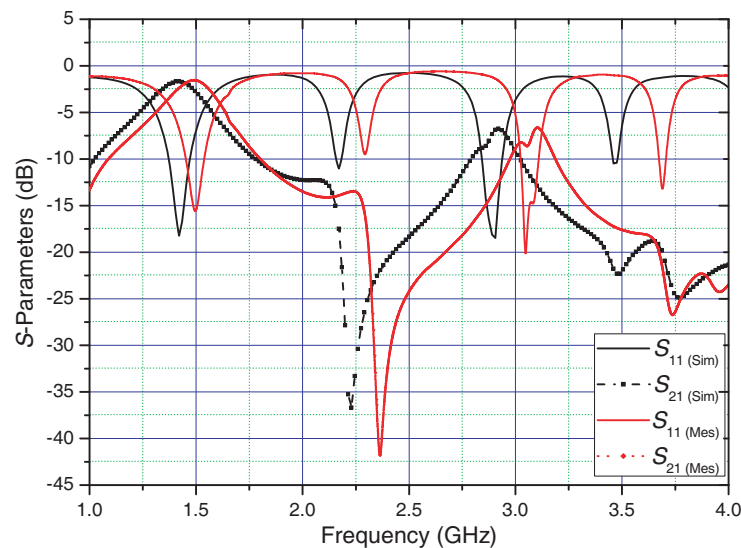


Figure 12. Simulated and measured S -parameters of the proposed BPF using IE3D simulator.

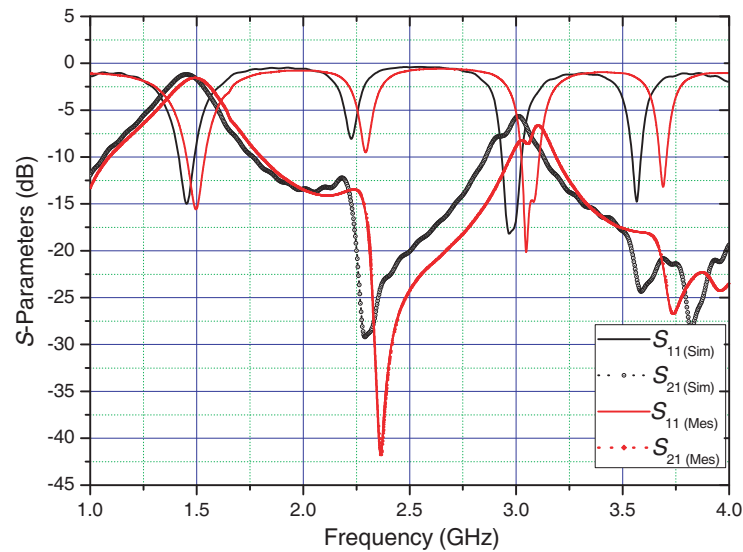


Figure 13. Simulated and measured S -parameters of the proposed BPF using CST simulator.

5. CONCLUSION

A novel compact harmonic-rejected BPF with stepped-impedance open stubs was proposed. The proposed BPF had the advantages of size reduction, simple structure and low cost. The proposed structure incorporated stubs and orthogonal feeding lines on the same area. Transmission zeros were controlled by curve perimeter and stubs' lengths according to the available space. Ring resonator's eigenvalue equation was solved and a design curve was obtained. Conventional ring resonator based BPF had two major disadvantages, big size and harmonics appearance. The conventional ring resonator based BPF size problem was solved by using second order Sierpinski curve, and a size reduction of 71% was obtained. New transmission zero was introduced at 3.84 GHz by adding two identical stepped-impedance open stubs. Rejection of -6.7 dB was obtained for the proposed BPF instead of -1.7 dB for the conventional one. The proposed BPF prototype was fabricated using low cost FR4 material. The proposed BPF insertion and return losses were measured and compared with simulated ones, and good agreement was obtained. The proposed BPF is operated at L-band frequency spectrum. In Europe, L band is used for terrestrial communications networks. In United States, L band is used for telemetry and digital audio broadcasting. The main limitation of the proposed structure is the narrow passband of the bandpass filter. This limitation may be solved by adding another resonator and considering the coupling between the main resonator and the new incorporated one.

REFERENCES

1. Chang, K., *Microwave Ring Circuits and Antennas*, New York, Wiley, 1996.
2. Kundu, A. C. and I. Awai, "Control of attenuation pole frequency of a dual-mode microstrip ring resonator bandpass filter," *IEEE Transactions on Microwave Theory and Techniques*, Vol. 49, No. 6, 1113–1117, 2001.
3. Wolff, I., "Microstrip bandpass filter using degenerate modes of a microstrip ring resonator," *Electronics Letters*, Vol. 8, No. 12, 302–303, 1972.
4. Chang, K., S. Martin, F. Wang, and J. L. Klein, "On the study of microstrip ring and varactor-tuned ring circuits," *IEEE Transactions on Microwave Theory and Techniques*, Vol. 35, No. 12, 1288–1295, 1987.

5. Hsieh, L. H. and K. Chang, "Compact, low insertion-loss, sharp-rejection, and wide-band microstrip bandpass filters," *IEEE Transactions on Microwave Theory and Techniques*, Vol. 51, No. 4, 1241–1246, 2003.
6. Sun, S. and L. Zhu, "Wideband microstrip ring resonator bandpass filters under multiple resonances," *IEEE Transactions on Microwave Theory and Techniques*, Vol. 55, No. 10, 2176–2182, 2007.
7. Chiou, Y. C., J. T. Kuo, and J. S. Wu, "Miniaturized dual-mode ring resonator bandpass filter with microstrip-to-CPW broadside-coupled structure," *IEEE Microwave and Wireless Components Letters*, Vol. 18, No. 2, 97–99, 2008.
8. Chiou, Y. C., C. Y. Wu, and J. T. Kuo, "New miniaturized dual-mode dual-band ring resonator bandpass filter with microwave C-sections," *IEEE Microwave and Wireless Components Letters*, Vol. 20, No. 2, 67–69, 2010.
9. Lin, T. W., J. T. Kuo, and S. J. Chung, "Miniaturized dual-mode spiral-ring resonator bandpass filter," *IEEE Asia-Pacific Microwave Conference Proceedings (APMC)*, 1127–1129, 2012.
10. Lin, T. W., J. T. Kuo, S. C. Tang, and S. J. Chung, "Miniaturized dual-mode ring resonator bandpass filter with a wide passband," *IEEE International Wireless Symposium (IWS)*, 1–3, 2014.
11. Peh, T. and N. M. Mahyuddin, "Miniaturized broadside-coupled split ring resonator bandpass filter using capacitor loading," *IEEE Radio and Antenna Days of the Indian Ocean (RADIO)*, 1–2, 2016.
12. El-Shaarawy, H. B., F. Coccetti, R. Plana, M. El Said, and E. A. Hashish, "Compact bandpass ring resonator filter with enhanced wide-band rejection characteristics using defected ground structures," *IEEE Microwave and Wireless Components Letters*, Vol. 18, No. 8, 500–502, 2008.
13. Griol, A., D. Mira, A. Martinez, J. Marti, and J. L. Corral, "Microstrip multistage coupled ring bandpass filters using photonic bandgap structures for harmonic suppression," *Electronics Letters*, Vol. 39, No. 1, 68–70, 2003.
14. Wahab, N. A., M. K. M. Salleh, Z. I. Khan, N. E. A. Rashid, and K. A. Othman, "Single mode ring resonator with harmonic suppression," *IEEE International Symposium on Communications and Information Technologies (ISCIT)*, 294–298, 2014.
15. Dhanasekaran, D., "Harmonic suppression of bandpass filter using square CSRR," *IEEE International Conference on Innovations in Information, Embedded and Communication Systems (ICIIECS)*, 1–3, 2015.
16. Lin, T. W., J. T. Kuo, and S. J. Chung, "Bandpass filter with generalized multiple-mode ring resonator configuration," *IEEE International Microwave Symposium Digest (MTT)*, 1–3, 2012.
17. Kuo, J. T., and Lin, T. W., "Dual-mode Dual-Band Ring Resonator Bandpass Filter with Transmission Zeros," *IEEE Asia-Pacific Microwave Conference Proceedings (APMC)*, 1865–1870, 2010.
18. Luo, S., Zhu, L., and Sun, S., "A Dual-Band Ring-Resonator Bandpass Filter Based on Two Pairs of Degenerate Modes," *IEEE Transactions on Microwave Theory and Techniques*, Vol. 58, No. 12, 3427–3432, 2010.
19. Ma, Z., H. Sasaki, C. P. Chen, T. Anada, and Y. Kobayashi, "Design of a wideband bandpass filter using microstrip parallel-coupled dual-mode ring resonator," *IEEE Asia-Pacific Microwave Conference Proceedings (APMC)*, 21–24, 2010.
20. Kawai, K., H. Okazaki, and S. Narahashi, "Ring resonators for bandwidth and center frequency tunable filter," *IEEE European Microwave Conference*, 298–301, 2007.
21. Kawai, K., H. Okazaki, and S. Narahashi, "Center frequency, bandwidth, and transfer function tunable bandpass filter using ring resonator and J-inverter," *IEEE Microwave Conference EuMC*, 1207–1210, 2009.
22. Tu, W. H. and K. Chang, "Compact microstrip band stop filter using open stub and spur line," *IEEE Microwave and Wireless Components Letters*, Vol. 15, No. 4, 268–270, 2005.
23. Salleh, M. K. M., G. Prigent, O. Pigaglio, and R. Crampagne, "Quarter-wavelength side-coupled ring resonator for bandpass filters," *IEEE Transactions on Microwave Theory and Techniques*, Vol. 56, No. 1, 156–162, 2008.

24. Murakami, K. and S. Kitazawa, "Transient responses of voltage and current on ring resonator and traveling-wave loop directional filters," *IEEE Microwave Conference Proceedings (APMC), 2010 Asia-Pacific*, 1185–1188, 2010.
25. Sun, S. and L. Zhu, "Wideband microstrip ring resonator bandpass filter with asymmetrically-loaded stubs," *IEEE Asia-Pacific Microwave Conference*, 1–4, 2008.
26. Kim, C. H. and K. Chang, "Ultra-wideband (UWB) ring resonator bandpass filter with a notched band," *IEEE Microwave and Wireless Components Letters*, Vol. 21, No. 4, 206–208, 2011.
27. Kim, C. H. and K. Chang, "Wideband ring resonator bandpass filter with dual stepped impedance stubs," *IEEE International Microwave Symposium Digest (MTT)*, 229–232, 2010.
28. Meng, L., J. Xu, and M. Gao, "A novel Ultra-Wideband (UWB) ring resonator bandpass filter with improved in-band and out-of-band performance," *International Conference on Electronics, Communications and Control (ICECC)*, 4108–4110, 2011.
29. Wolff, I. and N. Knoppik, "Microstrip ring resonator and dispersion measurement on microstrip lines," *Electronics Letters*, Vol. 7, No. 26, 779–781, 1971.
30. Garg, R., I. Bahl, and M. Bozzi, *Microstrip Lines and Slotlines*, 3rd Edition, Artech House, USA, 2013.
31. Jarry, P. and J. Beneat, *Design and Realizations of Miniaturized Fractal Microwave and RF Filters*, John Wiley and Sons, 2009.
32. Hu, R., J. Li, and S. Fan, "A novel fractal folded-slot antenna using Sierpinski curves," *IEEE Singapore International Conference on Communication Systems (ICCS)*, 371–373, 2008.